The pivotal role of von Willebrand factor binding to platelet αIIbβ3 in stabilizing the formation of a platelet plug at sites of injury

Qizhen Shi,[1-4] Jeremy G. Mattson,[1] Patricia A. Morateck,[1] Pamela A. Christopherson,[1] Jocelyn A. Schroeder,[1-4] Scot A. Fahs,[1] Jessica Rapten,[1] Marie L. Schulte,[1] Hartmut Weiler,[1,2] Jieqing Zhu,[1,2] Sandra L. Haberichter,[1,2] Veronica H. Flood[1-4] and Robert R. Montgomery[1,2]

[1]Thrombosis and Hemostasis Program, Versiti Blood Research Institute; [2]Departments of Pediatrics, Cell Biology, Neurology and Anatomic, and Biochemistry, Medical College of Wisconsin; [3]Children's Research Institute, Children's Wisconsin and [4]Midwest Athletes Against Childhood Cancer Fund Research Center, Milwaukee, WI, USA

Correspondence: Q. Shi
qshi@versiti.org

Received: February 26, 2025.
Accepted: May 9, 2025.
Early view: May 22, 2025.

https://doi.org/10.3324/haematol.2025.287685

Abstract

The interaction between von Willebrand factor (VWF) and platelet αIIbβ3 is thought to be essential for clot formation at injury sites, but its biological properties remain poorly understood due to the complexity and overlap with other αIIbβ3 ligands. Here, we developed a novel binding assay using a recombinant αIIbβ3 headpiece to evaluate VWF-αIIbβ3 binding in plasma from 441 Zimmerman Program participants. The VWF:αIIbβ3 to VWF:Ag ratio was significantly lower in patients with type-1, 2A, and 2B VWD than healthy controls. We identified five index cases with the p.R2464C variant in the VWF-C-domain, where affected family members displayed significantly reduced VWF:αIIbβ3/VWF:Ag ratios. To investigate the function of the VWF-αIIbβ3 interaction, we created a mouse model ($VWF^{RGES/RGES}$) by altering the VWF-RGDS motif to RGES, which abolished VWF-αIIbβ3 binding. $VWF^{RGES/RGES}$ mice exhibited increased blood loss following lateral tail vein transection and reduced thrombus stability in a laser injury model, showing a 59-fold larger AUC for emboli compared to wild-type. However, initial bleeding times and outcomes of carotid artery injury were comparable. Overall, our VWF:αIIbβ3 binding assay is valuable for characterizing VWD, and the VWF^{RGES} mouse model underscores the physiological significance of the VWF-αIIbβ3 interaction, highlighting that VWF-αIIbβ3 interaction is crucial for stabilizing platelet plug formation at injury sites.

Introduction

von Willebrand factor (VWF) is a large multimeric glycoprotein that plays multiple roles in hemostasis and thrombosis.[1] At the site of injury, after being exposed to the subendothelial matrix and bound to collagens, VWF serves as a central player interacting with its counterpart platelets through receptors glycoprotein Ibα (GPIbα) and GPIIb/IIIa ($\alpha_{IIb}\beta_3$ integrin).[2,3] VWF binds to GPIbα during vascular injury, enabling platelet tethering and starting primary hemostasis. This activates platelets, linking VWF to $\alpha_{IIb}\beta_3$ integrin and interacting with collagen in the subendothelial matrix during secondary hemostasis.[4,5] The interaction between VWF and the $\alpha_{IIb}\beta_3$ integrin is critical in maintaining hemostasis by supporting platelet adhesion and aggregation at vascular injury sites.[6] While the importance of the interaction between VWF and $\alpha_{IIb}\beta_3$ is recognized, its biological properties remain poorly understood due to the complex and dynamic nature of VWF-$\alpha_{IIb}\beta_3$ interaction, influenced by factors like blood flow shear rates, platelet activation,[7] and competition with other $\alpha_{IIb}\beta_3$ ligands, such as fibrinogen.[8] Disentangling VWF's specific contributions from other ligands that bind to the $\alpha_{IIb}\beta_3$ integrin is particularly challenging, making it difficult to fully understand how this interaction influences platelet plug formation and hemostatic function.[9,10] A significant challenge in studying VWF-$\alpha_{IIb}\beta_3$ interactions lies in the transient, activation-dependent nature of the binding. VWF only binds to $\alpha_{IIb}\beta_3$ when platelets are activated, leading to necessary conformational changes.[11] This process is further complicated because fibrinogen, the most abundant coagulation protein in the blood, competes with VWF for binding to the same $\alpha_{IIb}\beta_3$ receptor.[12] VWF binds to platelet-GPIb and increases at injury sites attached to collagen, complicating this interaction. It also undergoes shear-dependent changes, unfolding to expose binding domains that interact with platelet receptors.[13]

In addition to these biochemical challenges, experimental systems often fail to capture the dynamic flow conditions

under which VWF-$\alpha_{IIb}\beta_3$ interactions are most relevant.[14] Flow-based *in vitro* assays or microfluidic devices are needed to simulate physiological conditions accurately, but they are technically demanding. A cell-based assay utilizing $\alpha_{IIb}\beta_3$-stably-expressed on HEK293 demonstrated impaired binding to recombinant VWF (rVWF) with certain variants in the C-domains; however, it was ineffective for plasma samples.[15] Reliable assays to measure VWF's binding to $\alpha_{IIb}\beta_3$ are essential for understanding how mutations in VWF affect this interaction and improving diagnostics for von Willebrand disease (VWD). *In vivo* models that isolate VWF's role in this binding without fibrinogen interference can provide important tools to investigate the significance of this interaction in platelet plug formation and thrombus stability.

In this study, we developed a novel ELISA-based assay using recombinant $\alpha_{IIb}\beta_3$ headpiece to assess VWF binding in plasma samples from VWD subjects enrolled in the Zimmerman Program. We then created a mouse model with the VWF-RGES mutation to disrupt the RGD-dependent VWF-$\alpha_{IIb}\beta_3$ binding. Utilizing these tools, we systematically evaluated the impact of the VWF-$\alpha_{IIb}\beta_3$ interaction on hemostasis. Our results provide new insights into the role of VWF-$\alpha_{IIb}\beta_3$ binding in stabilizing platelet aggregates, contributing to a deeper understanding of hemostatic mechanisms and bleeding disorders.

Methods

The details of antibodies and reagents, as well as the methods and statistics used in this study, are provided in the *Online Supplementary Appendix*.

Patient populations and phenotype characterization

A total of 441 subjects, including VWD index cases and healthy controls (HC), were initially analyzed from clinical hematology centers as part of the Zimmerman Program for the Molecular and Clinical Biology of VWD[16] (see *Online Supplementary Appendix*). Informed consent was obtained, and the study was approved by the Institutional Review Board. Bleeding scores were assessed using ISTH-BAT.[17] Full exonic Sanger sequencing of the VWF gene identified variants in index cases, and targeted sequencing confirmed these variants in family members. Central laboratory VWF testing was also conducted to validate phenotypic diagnoses as reported.[18,19]

VWF-$\alpha_{IIb}\beta_3$ binding activity assay

The biological function of VWF in binding to $\alpha_{IIb}\beta_3$ was quantified by our novel ELISA-based assay using an antibody-captured recombinant human $\alpha_{IIb}\beta_3$ (rh-$\alpha_{IIb}\beta_3$) headpiece[20] (Figure 1A). The anti-human GPIIIa monoclonal antibody (MoAb) AP-3 was coated on a 96-well plate to capture rh-$\alpha_{IIb}\beta_3$. Plasma samples were heated to 56°C for 15 minutes (min), centrifuged to remove fibrinogen, and diluted heat-defibrinated plasma (HDP) samples were incubated for one hour (hr). Biotinylated anti-hVWF antibody AVW15 detected bound human VWF (hVWF). Two protocols determined mouse VWF:$\alpha_{IIb}\beta_3$ binding: one with rh-$\alpha_{IIb}\beta_3$ (mVWF:h$\alpha_{IIb}\beta_3$) and another with recombinant mouse $\alpha_{IIb}\beta_3$ (mVWF:m$\alpha_{IIb}\beta_3$). A biotinylated anti-VWF antibody (Dako) detected bound mVWF.

Generation of von Willebrand disease with RGES variant mouse models

All animal studies were performed according to protocols approved by the Institutional Animal Care and Use Committee of the Medical College of Wisconsin. The change of *VWF* c.7527T>A (p.Asp2509Glu), which converts the RGDS motif to RGES and impacts VWF binding to activated platelets as reported in an *in vitro* study,[21] was introduced into cloned mVWF-cDNA using a CRISPR-Cas9 strategy[22] to create an RGES-VWD mouse model. $VWF^{RGES/+}$ offspring were crossed to develop the $VWF^{RGES/RGES}$ model. $VWF^{RGES/RGES}$ mice were crossed with fibrinogen deficient ($Fib^{-/-}$)[23] or γ-chain variant ($Fib^{\gamma\Delta5/\gamma\Delta5}$)[24] mice to generate $Fib^{-/-}VWF^{RGES/RGES}$ and $Fib^{\gamma\Delta5/\gamma\Delta5}VWF^{RGES/RGES}$ mice.

von Willebrand factor antigen and von Willebrand factor-collagen binding activity assays

Mouse blood samples were collected and plasma was isolated as reported.[25] von Willebrand factor antigen (VWF:Ag) levels in mouse plasma were determined by ELISA.[26] For human VWF:Ag ELISA, anti-hVWF monoclonal antibodies (MoAb) were used. To determine the binding functions of RGES-VWF to collagen, we performed bindings assays for VWF with collagen-III (VWF:CB3) and collagen-IV (VWF:CB4) as reported[27-29] using samples from VWD subjects and $VWF^{RGES/RGES}$ mice.

Phenotypic assessments

The functional phenotype in VWF-RGES mice was assessed by *in vitro* rotational thromboelastometry (ROTEM) assay, native whole blood thrombin generation assay (nWB-TGA), and Venaflux following procedures described in our previous reports,[30-32] and by five *In vivo* injury models: 1) lateral tail vein transection (TVT) injury;[33] 2) tail-tip transection (TTT) by clipping 4 mm lengthwise for a 20 min bleeding test; 3) 6-hr tail bleeding test;[34] 4) $FeCl_3$-induced carotid artery injury; and 5) cremaster intravital laser injury.[35,36]

Results

The competency of a novel functional VWF/$\alpha_{IIb}\beta_3$ binding assay in characterizing subjects with various types of von Willebrand disease

To evaluate the binding capacity of VWF to the $\alpha_{IIb}\beta_3$ complex, we developed a novel functional assay using a recombinant $\alpha_{IIb}\beta_3$ headpiece: VWF:$\alpha_{IIb}\beta_3$ (Figure 1A). The rh-$\alpha_{IIb}\beta_3$ binds to HDP samples from human, rat, and mouse wild-type (WT) VWF but not to mutant VWF from RGES mice, demonstrating

RGD-dependent binding (*Online Supplementary Figure S1*). The ratio of VWF:$\alpha_{IIb}\beta_3$ to VWF:Ag was used to characterize our VWD cohorts enrolled in the Zimmerman Program.[16] The VWF:$\alpha_{IIb}\beta_3$/VWF:Ag ratio in the normal healthy control (HC) group was 0.87±0.25, which was significantly higher compared to those in the low VWF (LVWF), type-1, type-2A, type-2B, and type-2M-VWD groups (Table 1, Figure 1B). The 5-95% range of the VWF:$\alpha_{IIb}\beta_3$/VWF:Ag ratio from HC was between 0.53-1.39. Using only subjects with normal multimers (HC, LVWF, and type-1-VWD), we observed that reduced VWF:$\alpha_{IIb}\beta_3$/VWF:Ag significantly correlated with lower VWF:Ag (Figure 1C). Using VWF:CB3 (VWF:Collagen-III [CB3] binding) as a surrogate for multimer size,[37] we found that low VWF:CB3/VWF:Ag (reflecting loss of HMW multimers)[37] correlates with lower VWF:$\alpha_{IIb}\beta_3$ binding in Zimmerman Index Cases (LVWF, type-1-VWD, and type-2-VWD) (Figure 1D).

We then used the VWF:$\alpha_{IIb}\beta_3$ assay to test the binding ability of VWF from VWD subjects with a variant in the $\alpha_{IIb}\beta_3$-binding region (VWF-C-domain). We identified five index cases with p.R2464C in the VWF-C-domain; four were phenotypically diagnosed as LVWF and one as type-1-VWD. All p.R2464C subjects had a decreased VWF:$\alpha_{IIb}\beta_3$/VWF:Ag ratio ≤0.5 but had normal VWF multimers. Since our p.R2464C Index cases were clinically diagnosed as either LVWF or type-1-VWD, we compared the characteristics of subjects with the p.R2464C variant to type-1-VWD/LVWF. There was no difference in VWF activity as determined by VWF:GPIbM binding or VWF:Rco[38] between subjects with p.R2464C and type-1-VWD/LVWF cohort (Table 2). Compared to subjects with type-1-VWD/LVWF, the VWF:Ag level in the group with p.R2464C variant was similar (Figure 2A). However, the functional VWF:$\alpha_{IIb}\beta_3$ binding level and VWF:$\alpha_{IIb}\beta_3$/VWF:Ag ratio in the p.R2464C group were significantly lower than in the type-1-VWD/LVWF group, including subjects with other C-domain variants (Figure 2A). We then compared unaffected (N=6) *versus* affected (N=5) family members and index cases (N=4) within the four families with only the p.R2464C variant (one family had another VWF variant in addition to p.R2464C). In these families, we found the VWF:$\alpha_{IIb}\beta_3$/VWF:Ag ratio in members with the R2464C variant was significantly lower than in unaffected family members (0.37±0.06 *vs*. 0.88±0.57, P<0.01) (Figure 2B). The bleeding score in affected members was significantly higher than in family members without the R2464C variant (6±5.3 *vs*. 0.67±1.63, P<0.05) (Figure 2C).

These data demonstrated that the functional VWF-$\alpha_{IIb}\beta_3$ binding assay we established is valuable for the characterization of patients with VWD and for studying VWF:$\alpha_{IIb}\beta_3$ interactions *in vivo* in a mouse model.

Establishing a VWF-RGES model

To investigate the functional properties of the interaction between VWF and $\alpha_{IIb}\beta_3$, we developed a mouse model that directly alters the VWF-RGDS binding motif to VWF-RGES using a CRISPR/Cas9 strategy (*Online Supplementary Figure S2A*). We introduced variant RGES into cloned mouse VWF (mVWF) cDNA for mouse model development. Three lines of VWF^{RGES} mice carrying the c.7527T>A change with a similar phenotype were generated. Animals were genotyped using PCR and a diagnostic SacII site introduced in the RGES-VWF allele (*Online Supplementary Figure S2B*, C) from which the

Table 1. Comparison of the ratio of the von Willebrand factor's $\alpha_{IIb}\beta_3$ binding capacity to von Willebrand factor total antigen among various types of von Willebrand disease subjects.

	Healthy control	Low VWF	Type-1 VWD	Type-2A VWD	Type-2B VWD	Type-2M VWD	Type-2N VWD
N	84	162	75	50	37	22	11
VWF:$\alpha_{IIb}\beta_3$/ VWF:Ag, mean	0.87	0.70	0.57	0.29	0.38	0.75	0.95
P value (compared to HC)	-	0.0021	<0.0001	<0.0001	<0.0001	0.041	0.9999

HC: healthy controls; N: number; VWF:Ag: von Willebrand factor (VWF) total antigen; VWD: von Willebrand disease.

Table 2. The characteristics of family members with and without the p.R2464C variant in the Zimmerman Program.

Subjects (N)	Age in years, median (range)	VWF:Ag IU/dL, mean	VWF Activity IU/dL, mean	VWF Activity*/ VWF:Ag, mean	VWF:$\alpha_{IIb}\beta_3$ U/ dL, mean	VWF:$\alpha_{IIb}\beta_3$/ VWF:Ag	Total ISTH BS, median (range)
p.R2464C (9)	17 (5-50)	43	49	1.17	15	0.34	6 (0-18)
No p.R2464C (6)	18.5 (1-45)	58	63	1.09	62	1.08	0 (0-4)
Type 1/Low VWF (232)	15 (0-60)	40	46	1.15	27	0.66	5 (0-29)
Healthy control (84)	37 (18-65)	99	109	1.14	89	0.87	1 (0-8)

*von Willebrand factor (VWF) activity either VWF:GPIbM or VWF:Rco.[38] There is no difference in VWF activity (platelet binding) or bleeding score between subjects with p.R2464C and type-1-VWD/low VWF cohort. VWF:Ag: VWF total antigen; ISTH BS: International Society on Thrombosis and Hemostasis bleeding score.

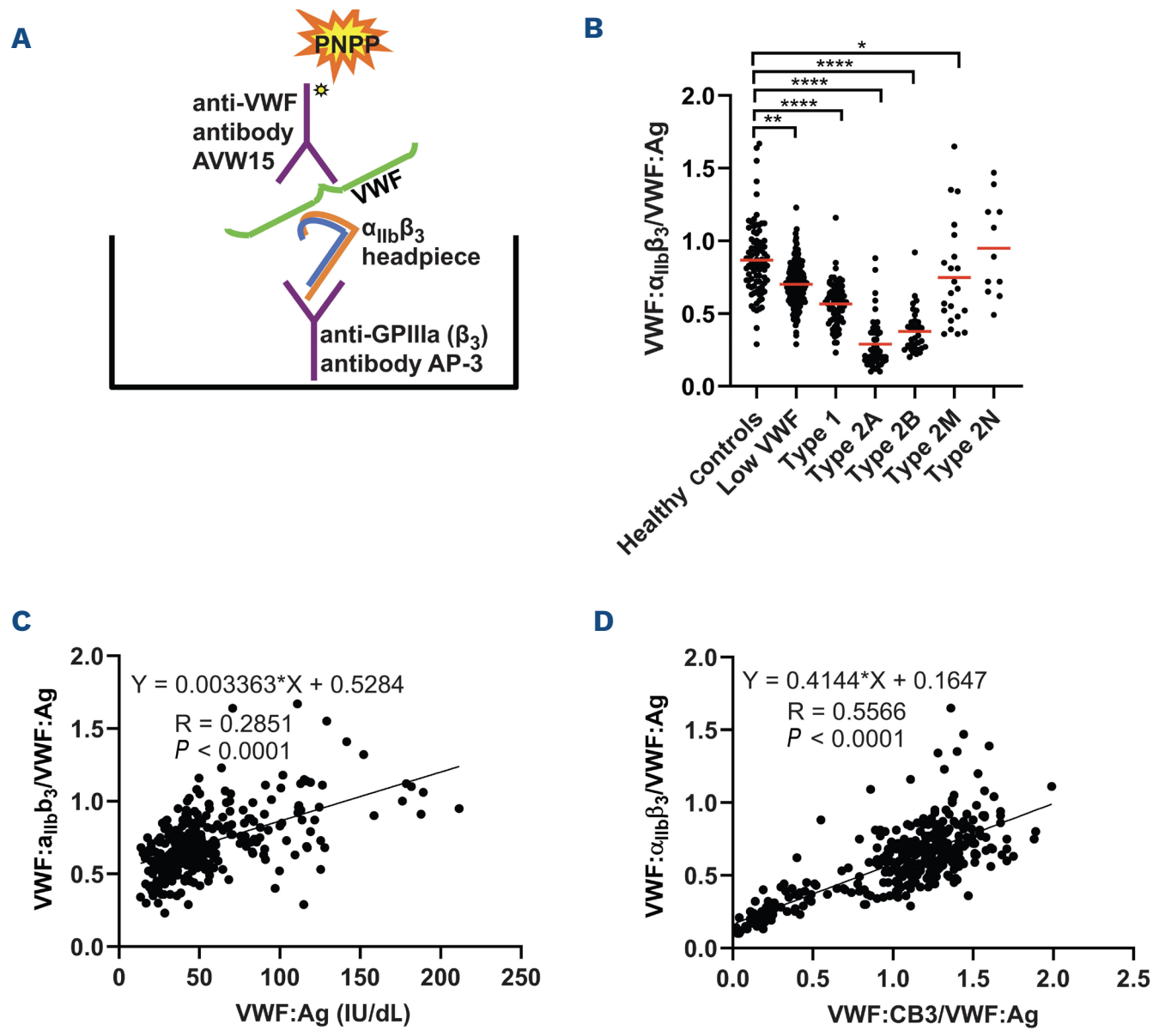

Figure 1. Developing the functional assay to assess von Willebrand factor binding to platelet $\alpha_{IIb}\beta_3$ integrin in human plasma from subjects with von Willebrand disease. For the functional von Willebrand factor (VWF) binding to platelet $\alpha_{IIb}\beta_3$ integrin (VWF:$\alpha_{IIb}\beta_3$) binding assay, an anti-human GPIIIa (β_3) monoclonal antibody (AP-3) was coated on a 96-well ELISA plate and recombinant human $\alpha_{IIb}\beta_3$ headpiece was captured from a 0.25 μg/mL solution. Plasma samples from individuals enrolled in the Zimmerman Program were heated, defibrinated, and incubated with the antibody captured $\alpha_{IIb}\beta_3$. The unbound VWF was washed off, and the remaining $\alpha_{IIb}\beta_3$-bound human VWF was detected using biotinylated mouse anti-human VWF monoclonal antibody, AVW15, and p-nitrophenyl phosphate (PNPP) was used as the substrate. The standard curve was constructed by measuring VWF binding from serially diluted heat-defibrinated plasma from SSC/ISTH Lot#5. The levels of VWF antigen (VWF:Ag) and VWF binding to collagen III (VWF:CB3) in plasmas were determined by ELISA. Human plasma from SSC/ISTH lot#5 was used as the standard. (A) Schematic diagram of the VWF:$\alpha_{IIb}\beta_3$ binding activity assay. (B) The ratio of functional VWF:$\alpha_{IIb}\beta_3$ binding activity to VWF:Ag level [VWF:$\alpha_{IIb}\beta_3$/VWF:Ag] in subjects with various types of von Willebrand disease (VWD). (C) The correlation between the VWF:$\alpha_{IIb}\beta_3$/VWF:Ag ratio and the VWF:Ag level in samples from index cases of patients with type-1-VWD, and low-VWF levels (LVWF), as well as the healthy controls (HC); N=321. (D) The correlation between the VWF:$\alpha_{IIb}\beta_3$/VWF:Ag ratio and the VWF:CB3/VWF:Ag ratio in samples from the VWD Index patients; N=357. (B-D) Each data point represents one subject. These results demonstrate that our novel functional VWF:$\alpha_{IIb}\beta_3$ binding activity assay utilizing the mobilized recombinant human $\alpha_{IIb}\beta_3$ headpiece-mediated ELISA is valuable for characterizing various types of VWD.

WT-VWF allele produced a 783-bp band, while the RGES-VWF mutation resulted in 579-bp and 204-bp bands. Thus, $VWF^{+/+}$ mice showed only the 783-bp fragment, homozygous $VWF^{RGES/RGES}$ mice had both the 579-bp and 204-bp fragments, and heterozygous $VWF^{RGES/+}$ mice displayed all three fragments (*Online Supplementary Figure S2C*).

To characterize VWF^{RGES} animals, we used ELISA[25,26,39] to determine plasma VWF:Ag levels and our new VWF:$\alpha_{IIb}\beta_3$ binding assay. The plasma VWF:Ag level in $VWF^{RGES/RGES}$ mice was 119.32±37.96U/dL, comparable to $VWF^{RGES/+}$ and $VWF^{+/+}$ mice (Figure 3A). The $VWF^{RGES/RGES}$ mice had normal levels of plasma FVIII (*data not shown*). Notably, no mVWF bound to rh-$\alpha_{IIb}\beta_3$ in HDP samples from the $VWF^{RGES/RGES}$ group, while the $VWF^{RGES/+}$ group showed a binding level of 50.57±17.82U/dL, significantly lower than in the $VWF^{+/+}$ group (98.14±40.64U/dL) (Figure 3B). Despite impaired binding to $\alpha_{IIb}\beta_3$, VWF^{RGES} mice displayed similar binding to collagen-III and collagen-IV compared to $VWF^{+/+}$ mice (*Online Supplementary Figure S3A-D*). VWF^{RGES} mice had normal VWF multimers (Figure 3C) and FVIII:C levels (*Online Supplementary Figure S3E*). To eliminate fibrinogen's interference with VWF binding to $\alpha_{IIb}\beta_3$, we crossed VWF^{RGES}

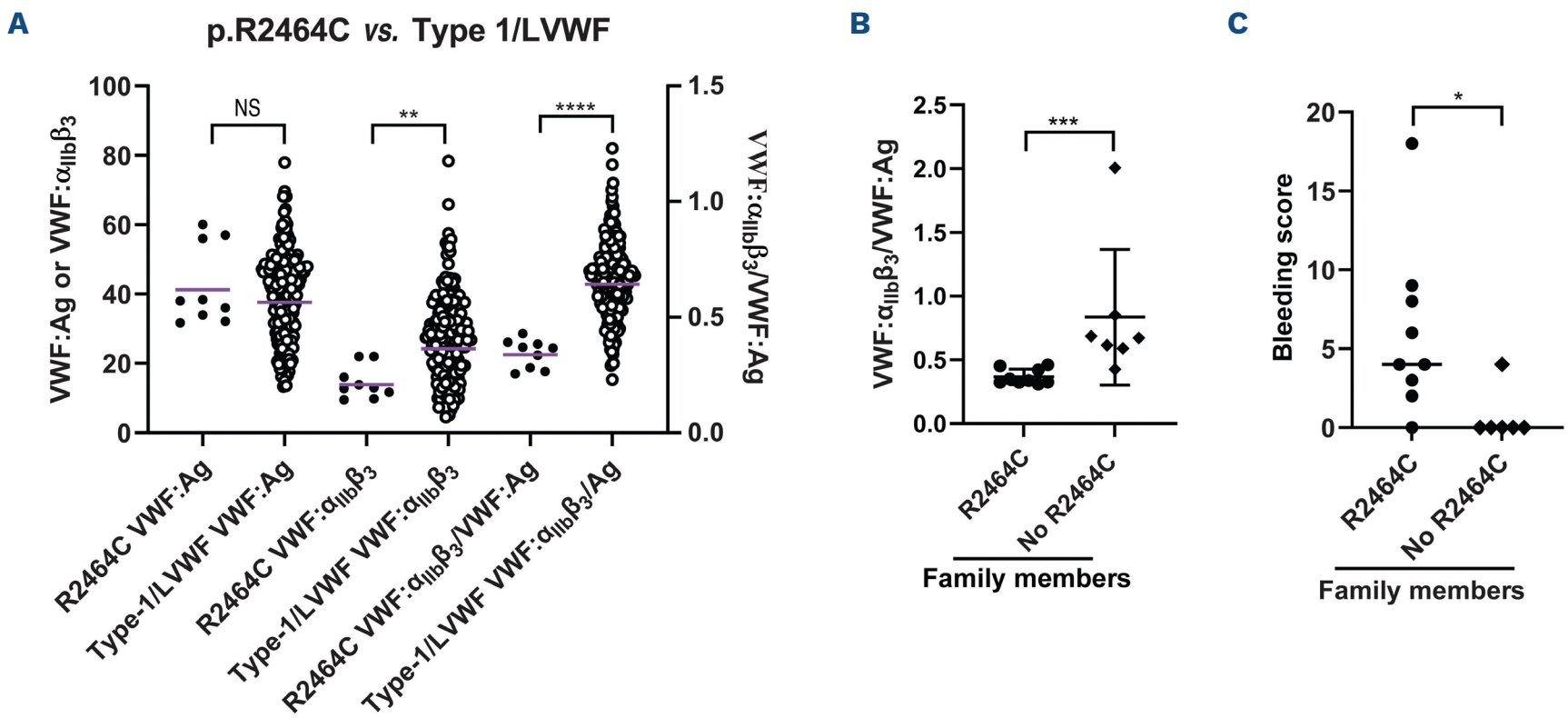

Figure 2. Using functional von Willebrand factor binding to platelet αIIbβ3 integrin activity assay to characterize von Willebrand disease subjects with the R2464C variant. For the functional VWF:$\alpha_{IIb}\beta_3$ binding assay, an anti-human GPIIIa (β3) monoclonal antibody (AP-3) was coated on a 96-well plate, and recombinant human $\alpha_{IIb}\beta_3$ headpiece was captured. Plasma samples from the Zimmerman Program were heat-defibrinated and incubated with the antibody-captured $\alpha_{IIb}\beta_3$. After washing away the unbound von Willebrand factor (VWF), the remaining bound VWF was detected using a biotinylated mouse anti-human VWF antibody (AVW15) and p-nitrophenyl phosphate (PNPP) as the substrate. The standard curve was established with VWF binding from serially diluted heat-defibrinated plasma from SSC/ISTH Lot #5. VWF antigen (VWF:Ag) levels were quantitated by ELISA and human plasma from SSC/ISTH lot#5 was used as the standard. (A) The levels of VWF:Ag and VWF:$\alpha_{IIb}\beta_3$, and the ratio of VWF:$\alpha_{IIb}\beta_3$/VWF:Ag in patients with p.R2464C variant compared to those with type-1-VWD and LVWF. (B) The ratio of VWF:$\alpha_{IIb}\beta_3$/VWF:Ag in the affected family members from our Index Cases with p.R2464C variant compared to those in unaffected members. (C) The bleeding score of the affected family members from our Index Cases with p.R2464C variant compared to those in unaffected members. *P<0.05; **P<0.01; ****P<0.0001; NS: no significant difference between the two groups. (A-C) Each data point represents one subject. These results demonstrate that our functional VWF:$\alpha_{IIb}\beta_3$ binding activity assay is viable in quantitating the capacity of VWF in binding to $\alpha_{IIb}\beta_3$ integrin, and the ratio of VWF:$\alpha_{IIb}\beta_3$/VWF:Ag is a valuable parameter for clinical diagnosis of von Willebrand disease (VWD).

mice onto a Fib$^{-/-}$ background. The mVWF:m$\alpha_{IIb}\beta_3$ binding activity in non-defibrinated plasma was 91.84±45.45U/dL in the Fib$^{-/-}$ group (Figure 3D). In the Fib$^{-/-}$VWF$^{RGES/+}$ group, it was 18.96±7.94U/dL, while no binding was detected in the Fib$^{-/-}$VWF$^{RGES/RGES}$ and Fib$^{-/-}$VWF$^{-/-}$groups. Overall, the VWF^{RGES} model has normal plasma VWF levels and multimers but lacks $\alpha_{IIb}\beta_3$ binding activity while still effectively binding to collagen-III and IV.

Assessment of the functional properties VWF-RGES in whole blood assays of VWF^{RGES} model mice

To determine how VWF-RGES affects hemostatic properties in whole blood, we used native ROTEM[30] and nWB-TGA.[31] There are no significant differences in any parameters from ROTEM and nWB-TGA between the VWF$^{RGES/RGES}$ group and the VWF$^{+/+}$ and VWF$^{RGES/+}$ groups (*Online Supplementary Figures S4* and *S5*). To assess the effect of VWF-RGES on platelet adhesion to collagen under flow conditions, we used the VenaFlux microfluidic platform on the collagen-III-coated chip[27] to analyze whole blood from various mouse models: Fib$^{\gamma\Delta5/\gamma\Delta5}VWF^{RGES/RGES}$, Fib$^{-/-}VWF^{RGES/RGES}$, Fib$^{-/-}VWF^{-/-}$, Fib$^{-/-}$, and C57BL/6J-WT. Under shear stress of 67.5dyn/cm², platelet coverage on the collagen-III-coated chip increased over time, reaching 40-50% by the study's end, except for the Fib$^{-/-}$VWF$^{-/-}$ group, which showed negligible adhesion (*Online Supplementary Figure S6A, B).*

We tested the anti-GPIIb/IIIa antibody LeoH4, blocking the $\alpha_{IIb}\beta_3$ receptor, to determine if collagen adhesion occurred. No adhesion was found in the VWF$^{-/-}$ group, but platelet coverage in the WT/Leo.H4 group matched the WT/IgG and WT/saline controls, as well as the Fib$^{-/-}$ group. Interestingly, platelets in the WT/Leo.H4 group adhered as single entities rather than aggregates, unlike the WT/IgG and WT/saline groups that showed platelet aggregates (*Online Supplementary Figure S6C, D*).

Together, these data demonstrate that even though the VWF-$\alpha_{IIb}\beta_3$ interaction is impaired in RGES-VWD blood, the hemostatic parameters determined by ROTEM and nWB-TGA are unaffected, and platelets can still effectively adhere to collagen for thrombus formation through another VWF-mediated pathway in the Venaflux model.

Assessment of the *in vivo* bleeding phenotypes in VWF^{RGES} model mice

To investigate how RGES-VWF affects the bleeding phenotype in mice, we used five *In vivo* injury models: 1) TVT;[33] 2) TTT;[22] 3) 6-hr tail bleeding test;[34] 4) $FeCl_3$-induced injury;[40] and 5) cremaster laser injury.[35] In the blinded TVT injury model, no significant differences in primary, rechallenge, or total bleeding time were found between the VWF$^{RGES/RGES}$ and

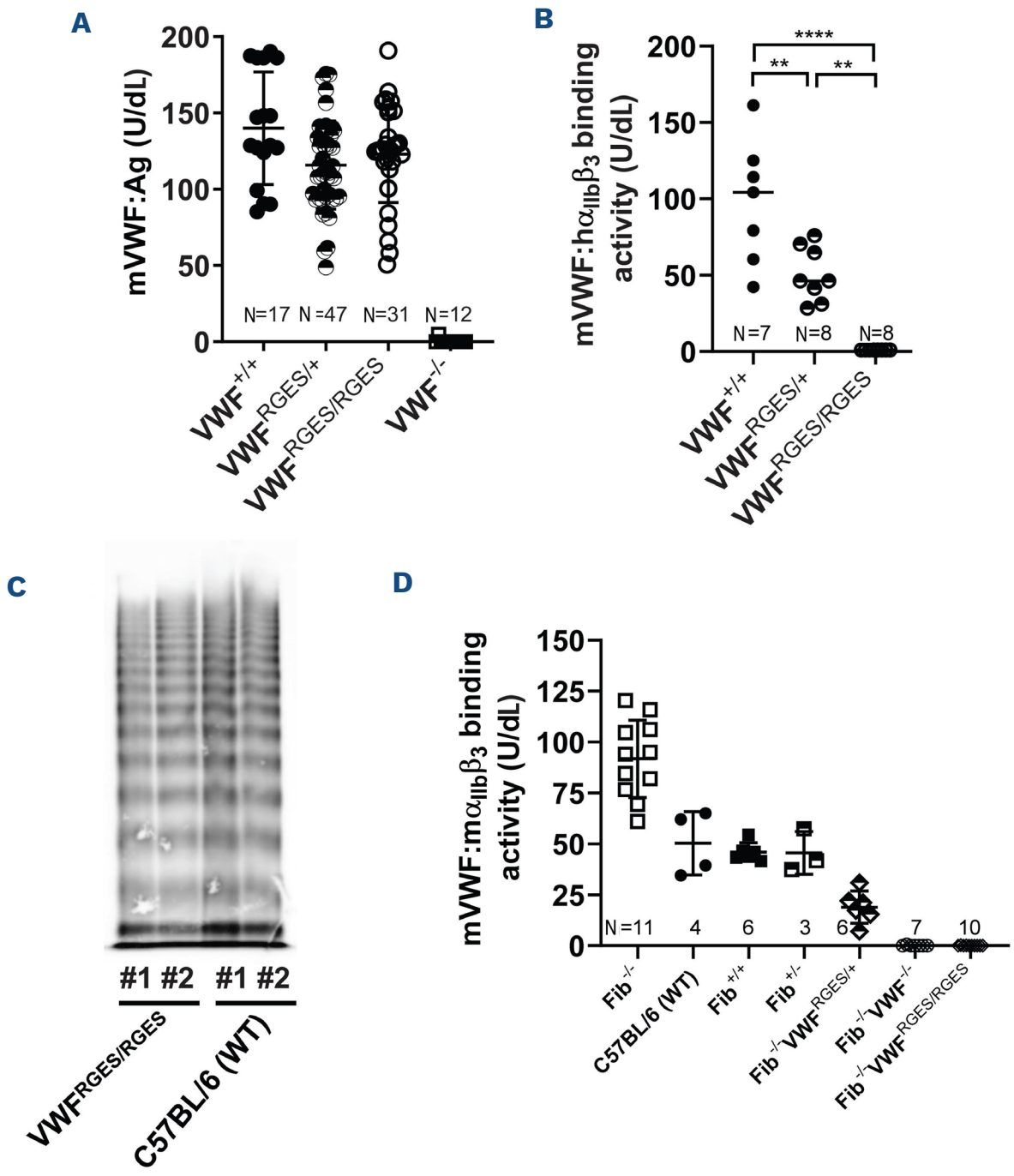

Figure 3. Characterization of von Willebrand factor and its functional binding activity to αIIbβ3 in RGES variant von Willebrand factor model mice. (A) Plasma von Willebrand factor (VWF) antigen (VWF:Ag) levels. Blood samples were collected from three lines of RGES variant von Willebrand disease (VWD) model (VWF^{RGES}) mice by tail bleeds using 3.8% sodium citrate as an anticoagulant, and plasmas were isolated for VWF assays. Plasmas from VWF$^{+/+}$ and VWF$^{RGES/+}$ littermates were used as parallel controls. Mouse VWF antigen (VWF:Ag) levels were determined by ELISA assay using anti-mouse VWF monoclonal antibody 344.2 for capture and biotin-conjugated rabbit anti-human VWF polyclonal antibody, Dako, that is known to cross-react with mouse VWF for detection. Plasma pooled from our wild-type C57BL/6J colony was used as the standard. Plasma from VWF$^{-/-}$ mice were used as a negative control. (B) The capacity of mouse VWF binding to recombinant human $\alpha_{IIb}\beta_3$ headpiece (mVWF:h$\alpha_{IIb}\beta_3$). Anti-human β3 monoclonal antibody AP3 was coated onto a 96-well plate to capture recombinant human $\alpha_{IIb}\beta_3$ from a 0.25 μg/mL solution. Plasma from VWF^{RGES} mice was heat-defibrinated and incubated with the antibody-bound h$\alpha_{IIb}\beta_3$. After washing away unbound mouse VWF, the $\alpha_{IIb}\beta_3$-bound mVWF was detected using ELISA reagents. A standard curve was created by measuring mVWF binding from serially diluted heat-defibrinated plasma from wild-type C57BL/6J mice. (C) The ability of RGES-VWF in multimerization. To examine if VWF in VWF$^{RGES/RGES}$ mice can fully multimerize, we ran VWF multimers on plasma samples from RGES mice. Plasma from C57BL/6 mice were run in parallel. (D) The capacity of mouse VWF binding to recombinant murine $\alpha_{IIb}\beta_3$ (mVWF:m$\alpha_{IIb}\beta_3$). To eliminate fibrinogen interference, some VWF^{RGES} mice were crossed onto a fibrinogen-deficient (Fib$^{-/-}$) background. Anti-mouse CD41 (αIIb) monoclonal antibody was coated on a 96-well plate to capture recombinant murine $\alpha_{IIb}\beta_3$ (m$\alpha_{IIb}\beta_3$) at 5 μg/mL. Undefibrinated mouse plasma samples from Fib$^{-/-}$VWF^{RGES} were added, allowing bound mVWF to be detected via ELISA after washing away unbound VWF. A standard curve was created from serially diluted pooled plasma from Fib$^{-/-}$ mice. Plasmas from C57BL/6, Fib$^{+/+}$, and Fib$^{+/-}$ mice were assayed as controls. (A, B, D) Each data point represents one mouse. ****P<0.0001. These results demonstrate that VWF-RGES mice have normal levels of plasma VWF but are incapable of binding mouse $\alpha_{IIb}\beta_3$ integrin.

C57BL/6J-WT groups (Figure 4A, B). However, the VWF$^{RGES/RGES}$ group experienced significantly higher blood loss during the rechallenge and total tests than the WT group, while the primary bleeding phase loss remained similar (Figure 4C). The VWF$^{-/-}$ group had a significantly longer bleeding time than the VWF$^{RGES/RGES}$ group, but no significant difference in blood loss was noted, regardless of phase.

In the TTT model, there were no significant differences in bleeding time and blood loss between the VWF$^{RGES/RGES}$ and WT groups. In contrast, the bleeding time and blood loss in the VWF$^{-/-}$ group were significantly different from those in the VWF$^{RGES/RGES}$ and WT groups (Figure 5A). In the 6-hr tail bleeding test, the percentage of remaining hemoglobin in the VWF$^{RGES/RGES}$ group was comparable to that in the WT group. Re-bleeds occurred in 2 of 6 VWF$^{RGES/RGES}$ mice but not in the WT animals during the test (Figure 6B). In the $FeCl_3$-induced carotid artery injury model, there was no significant difference in the occlusion time between the VWF$^{RGES/RGES}$ group and the C57BL/6J-WT group (Figure 5C).

Together, these data demonstrate that the VWF-RGES variant

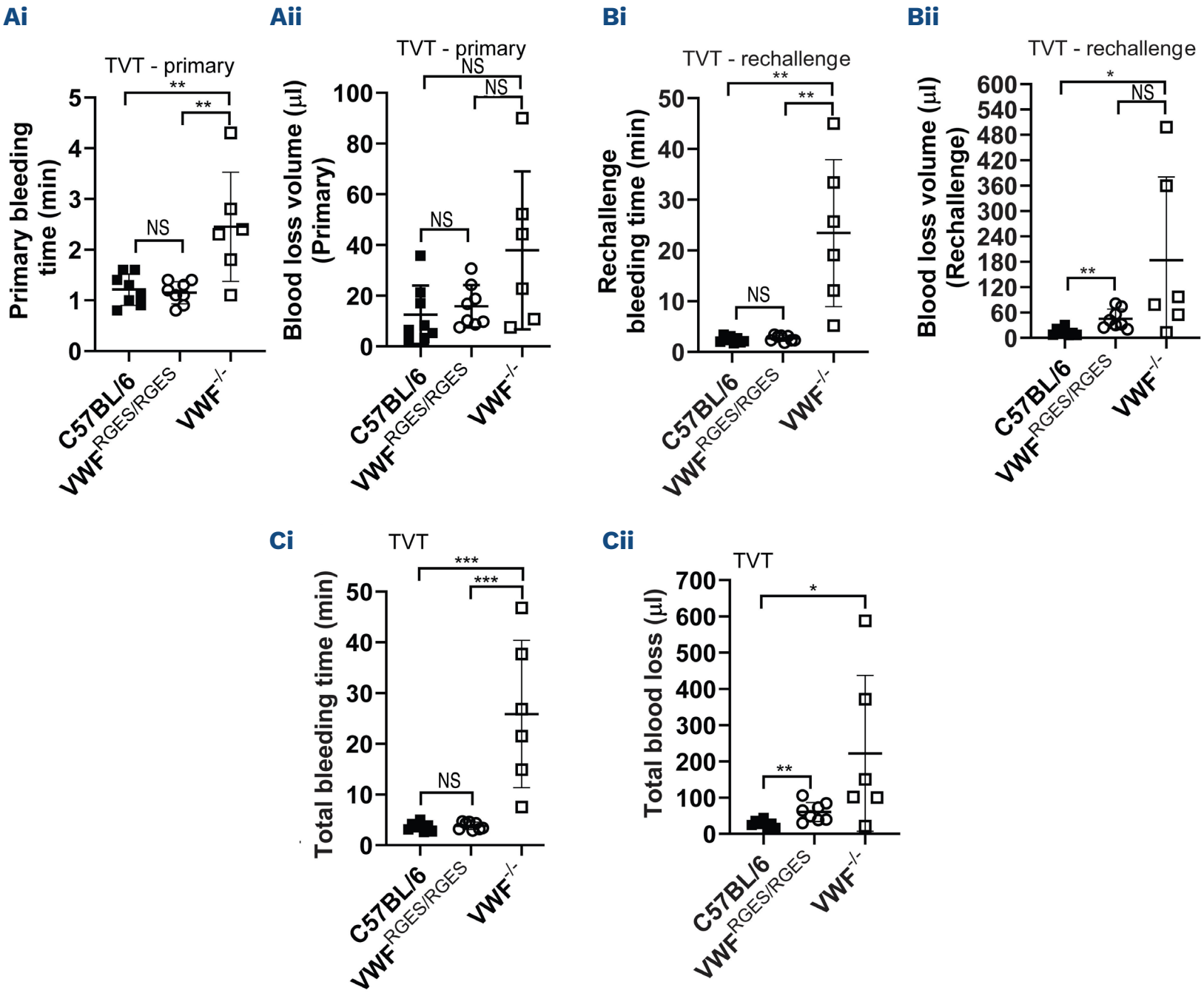

Figure 4. Assessment of the bleeding phenotype in RGES variant von Willebrand disease model mice using lateral tail vein transection injury model. RGES variant von Willebrand disease (VWF$^{RGES/RGES}$) model mice were anesthetized with isoflurane, and a 1-mm deep transection was performed in the left lateral tail vein at a 2.5 mm diameter, using an aluminum template to assess the bleeding phenotype. The tail was submerged in 14 mL of pre-warmed saline for 15 minutes (min). If bleeding stopped, the tail was removed from the saline; if not, it remained submerged for the full duration. Clotting was tested three times, and bleeding times were recorded. Blood loss was quantified by lysing red blood cells in 10 mL of distilled water and measuring hemoglobin at OD575 nm, with calculations based on a standard curve from the pooled blood of wild-type C57BL/6J mice. Total bleeding times and blood losses across the three re-challenges were combined. Mice from the wild-type C57BL/6J colony and VWF$^{-/-}$ served as controls. (Ai-Aii) Bleeding time (AI) and blood loss (Aii) during primary challenge. (Bi-Bii) Bleeding time (Bi) and blood loss (Bii) during re-challenges. (Ci-Cii) Total bleeding time (Ci) and blood loss (Cii) from primary and re-challenges. (A-C) Each data point represents one mouse. *P<0.005; **P<0.01; ***P<0.001; NS: no significant difference between the two groups. These results demonstrate that von Willebrand factor (VWF) with the RGES variant significantly affects blood loss during rechallenge bleeding tests, but it does not impact bleeding time, nor does it affect blood loss or bleeding time in the primary challenge. TVT: tail vein transection.

does not result in prolonged bleeding times regardless of arterial or venous injury models in mice. However, VWF$^{RGES/RGES}$ animals lost more blood in the TVT injury model than WT mice.

Assessment of the *in vivo* thromboembolism phenotypes in VWF^{RGES} model mice

We performed laser injury on cremaster arterioles to explore how the RGES variant of VWF affects clot stability. We quantified thrombus formation by measuring the fluorescence intensity of accumulated platelets and fibrin and monitored emboli downstream of the thrombus. The total fluorescence intensity of accumulated platelets in thrombi formed in the laser-injured cremaster arterioles was similar between the VWF$^{RGES/RGES}$ and WT groups (Figure 6A, B). However, the VWF$^{RGES/RGES}$ group displayed more fluctuations, with more numbers of drop-offs. The area under the curve (AUC) for platelet accumulation was comparable between the groups

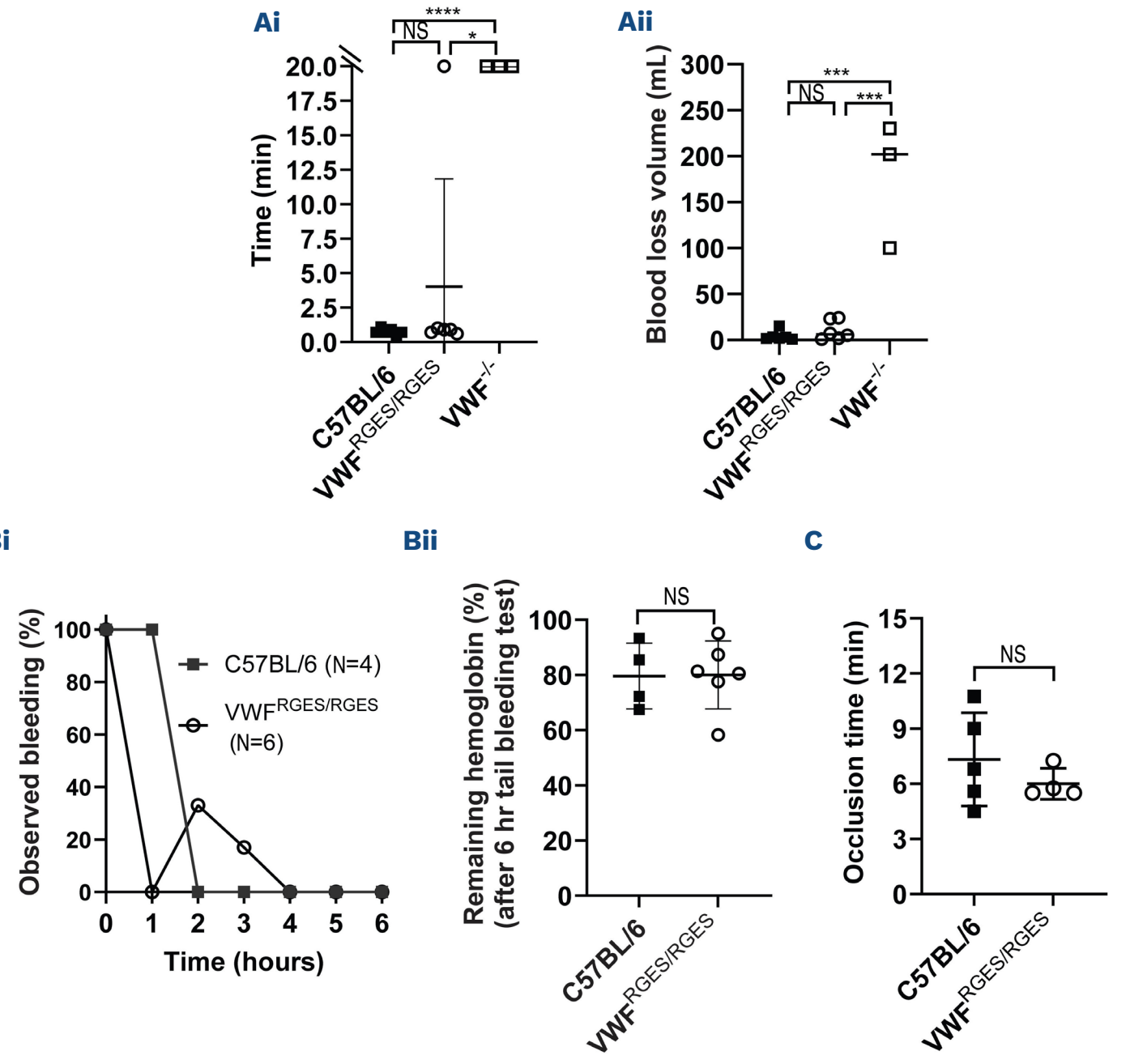

Figure 5. Assessment of the bleeding phenotype in RGES variant von Willebrand disease model mice using tail tip transaction and FeCl3-induced carotid artery injury models. (Ai-Aii) The tail bleeding test was performed by transecting a length of 4 mm of the tail tip. Animals were anesthetized with isoflurane, and 4 mm of the tail tip was clipped using a scalpel. The injured tail was submerged in 14 mL of pre-warmed saline for 20 minutes (min), during which bleeding times were recorded, and the results are shown in (Ai). Blood loss was measured by lysing red blood cells in 10 mL of dH_2O and analyzing hemoglobin at OD575 nm, using a standard curve from the pooled blood of wild-type C57BL/6J mice, and the results are shown in (Aii). Wild-type C57BL/6J and VWF$^{-/-}$ mice served as controls. (Bi-Bii). The 6-hour (hr) tail bleeding test was performed by transecting the tail tip at a diameter of 1.6 mm. Animals were anesthetized with isoflurane, and the tail tip was clipped by a scalpel. Animals were monitored hourly, and bleeding time was recorded and shown in (Bi). Fifty microliters of blood were collected before and after the test for blood counts, and the percentage of the remaining hemoglobin after the test was calculated; results are shown in (Bii). (C) $FeCl_3$-induced carotid artery injury model. The right carotid artery of ketamine-anesthetized mice was exposed. A 1x2 mm filter paper soaked in 15% ferric chloride was applied to the carotid artery for 3 minutes, then the surface of the artery was washed with PBS. Blood flow was monitored using a Doppler ultrasound flow probe. Time to occlusion of the carotid artery was recorded. (A-C) Each data point represents one mouse. *P<0.05; ***P<0.001; NS: no significant difference between the two groups. These results demonstrate that RGES variant von Willebrand disease (VWF-RGES) variant does not impact the bleeding phenotype in tail tip clipping tests and $FeCl_3$-induced carotid artery injury in VWF^{RGES} mice.

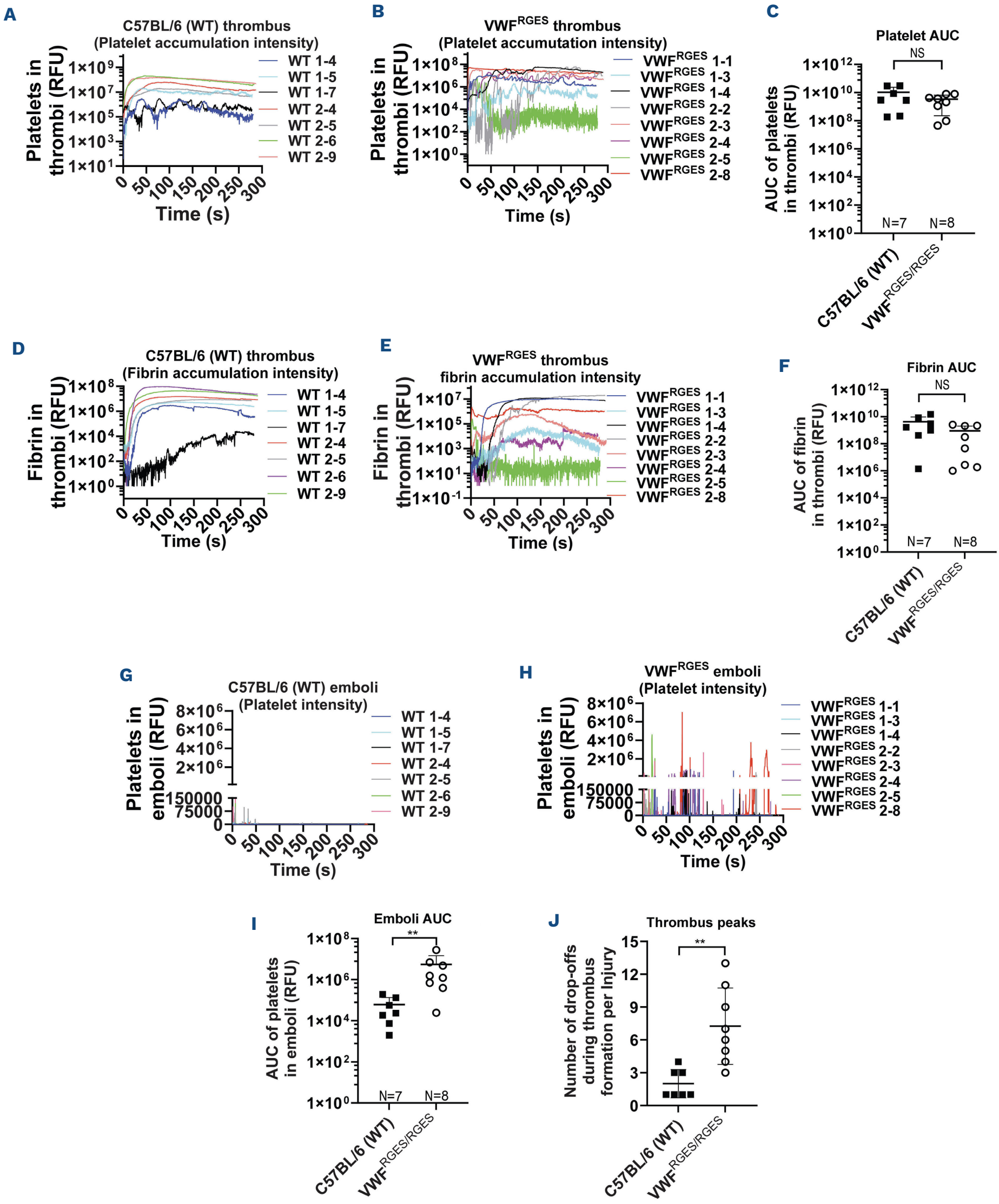

Continued on following page.

Figure 6. Assessment of the bleeding and embolism phenotype in RGES variant von Willebrand disease model mice using the cremaster intravital laser injury model. Male mice were anesthetized with a mixture of ketamine (75 mg/kg) and dexmedetomidine (0.5 mg/kg). The arterioles in the cremaster muscle were exposed. Fluorophore-labeled antibodies were injected retro-orbitally to label fibrin and platelets. Fibrin was labeled with an anti-fibrin monoclonal antibody conjugated to Alexa Fluor 647, while platelets were labeled with a rat anti-mouse GPIbβ monoclonal antibody conjugated to DyLight488. The vascular injury was induced using an enclosed pulsed laser, and the arteriolar thrombus formation and embolization were monitored and captured. The thrombus size was measured, and embolic events downstream were evaluated by creating an embolism mask that captured the full diameter of the vessel unaffected by the thrombus. Emboli were quantified by detecting labeled platelet aggregates, measuring the fluorescent signal over time as an area under the curve (AUC). (A) The fluorescent intensity of accumulated platelets in the thrombus formed in injured arterioles from C57BL/6J wild-type (WT) mice. (B) The fluorescent intensity of accumulated platelets in the thrombus formed in injured arterioles from RGES variant von Willebrand disease (VWF^{RGES}) mice. (C) A comparison of the AUC of platelet accumulation intensity in the thrombi formed after laser injury in VWF^{RGES} and WT mice. (D) The fluorescent intensity of accumulated fibrin in the thrombus formed in the injured arterioles from WT mice. (E) The fluorescent intensity of accumulated fibrin in the thrombus formed in the injured arterioles from VWF^{RGES} mice. (F) A comparison of the AUC of fibrin accumulation intensity in the thrombi formed after laser injury in VWF^{RGES} and WT mice. (G) The fluorescent intensity of embolized platelet plugs in WT mice. (H) The fluorescent intensity of embolized platelet plugs in VWF^{RGES} mice. (I) A comparison of the AUC of platelet accumulated intensity in emboli in VWF^{RGES} and WT mice. (J) A comparison of the drop-offs with a clear, sharp drop-off of platelet accumulation in thrombus during 300 seconds (s) after laser injury in VWF^{RGES} and WT mice. RFU: relative fluorescence units. ***P*<0.01; NS: no significant difference between the two groups.

(Figure 6C). Additionally, the total fluorescence intensity of fibrin in the thrombus showed no significant difference between the groups, although the median AUC for $VWF^{RGES/RGES}$ appeared lower than that for WT (Figure 6D-F).

In contrast, the accumulated platelets in the thrombi/clots formed in the cremaster laser injury model exhibited striking instability, with frequent fragmentation and embolization of thrombus material (platelet-plugs) observed downstream in $VWF^{RGES/RGES}$, but not WT mice (see *Online Supplementary Videos*). The rate of embolic platelet plugs downstream of the thrombus formed at the injury sites in the $VWF^{RGES/RGES}$ group was markedly higher than in the WT group (Figure 6G, H). The median AUC of emboli in the $VWF^{RGES/RGES}$ group was $1.39x10^6$ RFU, 59-fold higher than in the WT group ($2.34x10^4$ RFU) (Figure 6I). The number of drop-offs (peaks) during thrombus formation per injury of the cremaster arterioles in the $VWF^{RGES/RGES}$ group was 7.25±3.49, which was significantly higher than in the WT group (2±1.29, *P*<0.01) (Figure 6J).

Collectively, these observations reveal significant thrombus instability in $VWF^{RGES/RGES}$ mice, confirming that VWF's binding to platelet $\alpha_{IIb}\beta_3$ is crucial in stabilizing the formation of a platelet plug at sites of vascular injury.

Discussion

In this study, we developed a novel ELISA-based assay using the recombinant $\alpha_{IIb}\beta_3$ headpiece to determine VWF binding capacity to the $\alpha_{IIb}\beta_3$ integrin in VWD subjects' HDP samples. Furthermore, we generated the first mouse model with a defect at the RGD motif of VWF, resulting in a complete lack of binding capacity to the $\alpha_{IIb}\beta_3$ integrin. Our study provides critical insights into the biological properties of the interaction between VWF and the $\alpha_{IIb}\beta_3$ integrin with important applications in understanding and clinical diagnosis of VWD. Using our novel VWF-$\alpha_{IIb}\beta_3$ binding assay and the VWF-RGES mouse model, we elucidated the functional role of the VWF-$\alpha_{IIb}\beta_3$ interaction in hemostasis and thromboembolism. Our findings highlight that VWF-$\alpha_{IIb}\beta_3$ binding is essential for stabilizing platelet aggregates at injury sites in mice, complementing the well-characterized VWF-GPIbα pathway.

von Willebrand factor has a multidomain structure that interacts with various proteins, enabling its biological functions to encompass coagulation and a range of other important non-hemostatic processes.[1,13] While the contributions of other VWF domains, such as A1, A2, A3, and D, are well documented, variants in the C-domains remain poorly understood despite the presence of the important RGD motif known to interact with platelet $\alpha_{IIb}\beta_3$.[41] One of the major barriers to understanding the functional relevance of the C-domains has been the absence of a reliable assay to measure VWF-$\alpha_{IIb}\beta_3$ interactions.[42] The VWF:$\alpha_{IIb}\beta_3$ binding assay we developed demonstrated its viability by revealing significant reductions in VWF:$\alpha_{IIb}\beta_3$/VWF:Ag ratios in several VWD subtypes, including type-2A and type-1 individuals with the p.R2464C variant in the C-domains. It has been reported that among 12 known variants in the VWF-C-domain, 4 of them [p.Cys2257Arg, p.Gly2441Cys, p.Cys2477Tyr, and p.Pro2722Ala], but not p.Arg2464Cys (p.R2464C), exhibit reduced $\alpha_{IIb}\beta_3$ binding in a cell-based assay using GPIIb/IIIa-transfected-HEK293 cells and recombinant VWF.[15] Interestingly, none of those four variants with reduced $\alpha_{IIb}\beta_3$ binding were found among our Zimmerman Program subjects.

Using the recombinant $\alpha_{IIb}\beta_3$ headpiece, our ELISA-based assay effectively detects the binding capacity of VWF from both human and mouse plasma samples to integrin $\alpha_{IIb}\beta_3$. Previous studies have shown that employing $\alpha_{IIb}\beta_3$ purified from human platelets in ELISA or $\alpha_{IIb}\beta_3$-stably-expressed HEK293 cell-based assays is only effective for assessing VWF derived from cell culture supernatants (rVWF), but not for plasma samples.[15,43,44] Importantly, the impairment in p.R2464C was not evident by VWF multimer analysis and VWF:Ag in our Zimmerman Program subjects, highlighting our assay's ability to detect functional defects that may go

undiagnosed by conventional methods. The significance of the interaction between VWF and the $\alpha_{IIb}\beta_3$ receptor, especially regarding variants in the C-domain, has been understudied in relevant pathophysiological contexts. This is due to the complexity of the $\alpha_{IIb}\beta_3$ receptor, which comprises two proteins with multiple competitive binding ligands and whose binding affinity is influenced by inside-out signaling during platelet activation.[45] Our VWF:$\alpha_{IIb}\beta_3$ binding assay fills a valuable role in characterizing VWD, enabling the detection of subclinical VWF defects that could affect bleeding or thrombosis risk. Patients with VWD variants not identified by other functional tests, or those with a positive BAT score but normal VWF testing, should be considered for the VWF:$\alpha_{IIb}\beta_3$ test to rule out this type of VWD.

The clinical implication of this assay extends beyond diagnostics. It provides a framework for assessing the impact of variants in the C-domains, helping to refine genotype-phenotype correlations in VWD. This assay could also be valuable for personalized treatment strategies in clinical settings by identifying patients whose bleeding tendencies stem from impaired VWF-$\alpha_{IIb}\beta_3$ interactions. Furthermore, understanding how these variants influence thrombus formation can guide the development of novel therapies targeting VWF-integrin interactions, especially in cases where standard treatments are less effective. It has been reported that a gain-of-function variant of VWF affecting the VWF-C-domain can enhance platelet aggregation, thereby increasing the thromboembolism risk.[44,46] Our study suggests that measuring VWF-$\alpha_{IIb}\beta_3$ binding could improve diagnostic precision in VWD in patients, especially for patients with variants within the C-domain and other thrombotic disorders, by identifying patients with subclinical platelet function defects.

We found that the ratio of VWF:$\alpha_{IIb}\beta_3$/VWF:Ag in the type-1, 2A, and 2B VWD groups diagnosed using traditional VWF assays was significantly lower than in the healthy-control group from subjects recruited in the Zimmerman Program, indicating the capacity of VWF binding to platelet $\alpha_{IIb}\beta_3$ integrin is impacted in VWD with a variety of variants. These findings emphasize the clinical relevance of VWF-$\alpha_{IIb}\beta_3$ interaction in bleeding disorders. While the impact of impaired binding may be masked under normal conditions, it becomes apparent under certain stresses, such as microvascular injuries. We speculate that *VWF* variants may affect VWF-$\alpha_{IIb}\beta_3$ interaction by other mechanisms besides directly impairing the RGD motif. These may include: 1) altered VWF multimer structure; 2) changes to the glycan profile of VWF; and 3) VWF clearance variants. Clearly, both the quality and quantity of VWF impact the functional properties of VWF-$\alpha_{IIb}\beta_3$ interaction. Further studies on the applications of our VWF-$\alpha_{IIb}\beta_3$ binding assay in understanding how *VWF* variants in other domains besides the C4-domain where the binding motif is located affect the VWF-$\alpha_{IIb}\beta_3$ interactions are warranted.

To rigorously investigate the functional properties of the VWF-$\alpha_{IIb}\beta_3$ interactions, we developed a novel mouse model carrying a VWF mutation that completely abrogates binding to the $\alpha_{IIb}\beta_3$ integrin while exhibiting otherwise normal expression, multimerization, and functions. This model allows us to explore the contribution of this interaction in hemostasis and thromboembolism. These mice exhibited markedly increased platelet plug instability, as evidenced by frequent embolization in cremaster muscle arterioles following laser injury. In contrast, other bleeding models, like $FeCl_3$-induced carotid artery injury and tail tip amputation tests, did not reveal significant differences between the VWF^{RGES} and WT groups. Our results demonstrate that the binding of VWF to $\alpha_{IIb}\beta_3$ is essential for stabilizing aggregated platelets. This function is not redundant and cannot be compensated for by fibrinogen, even though fibrinogen is known to cross-link platelets by binding to the same $\alpha_{IIb}\beta_3$ receptor during thrombus formation at the injury site.

Platelets play fundamental roles in hemostasis following all types of vessel injury, but they are more critical in arterial than venous environments.[47-49] Interestingly, VWF^{RGES} mice lost significantly more blood than WT mice during the rechallenge TVT bleeding test. However, there were no significant differences in blood loss during the primary bleeding test nor in bleeding times between the two groups. Thus, the interaction between VWF and platelet $\alpha_{IIb}\beta_3$ integrin plays a more important role in stabilizing the clot formation in secondary hemostasis than platelet adherence in primary hemostasis. The results from various *In vivo* arterial and venous injury models demonstrate that VWF-$\alpha_{IIb}\beta_3$ interaction is crucial for thrombus stability under specific conditions, such as dynamic vascular flow or microvascular injury, but may not uniformly affect bleeding across all hemostatic scenarios. Therefore, we speculate that any variant impairing this interaction may increase the risk of thromboembolism, even with normal VWF expression levels. Indeed, it has been reported that the transient expression of VWF with a mutation in RGD (D2509G) (RGG-VWF), achieved under a liver-specific promoter through hydrodynamic injection of cDNA in $VWF^{-/-}$ mice, resulted in high plasma VWF levels. However, thrombus growth was delayed, and continuous embolization and occlusion times were significantly increased compared to WT-VWF transfected animals in the $FeCl_3$-induced injury model.[50] It remains unclear, though, to what extent these effects were caused by the loss of high molecular weight multimers of VWF introduced by hydrodynamic injection and ectopic hepatocyte expression in that study. Further research on the effect of VWF-$\alpha_{IIb}\beta_3$ interaction on thrombosis is necessary.

Our results also shed light on the redundant or complementary roles of fibrinogen and VWF in platelet aggregation and blood coagulation. Crossing the VWF variant mice onto a $Fib^{-/-}$ background confirmed that VWF binding to platelets becomes critical when fibrinogen is absent. No platelets from $Fib^{-/-}VWF^{-/-}$ whole blood could adhere to collagen. However, the binding of VWF to platelets and adherence onto collagen could still effectively occur in $Fib^{-/-}VWF^{RGES/RGES}$ mice, even though the VWF-$\alpha_{IIb}\beta_3$ interaction was impaired, as platelets can still bind to VWF

through the GPIα receptor. Our findings align with previous studies that demonstrate the complementary roles of fibrinogen and VWF, as well as the complexity of the intersecting pathways involving VWF and platelet integrin receptors in mediating platelet aggregation, especially under varying hemodynamic conditions.

In conclusion, our study shows that VWF-$\alpha_{IIb}\beta_3$ interactions are essential for platelet plug stability, especially under flow conditions affecting thrombus integrity. Our VWF-RGES mouse model combined with the VWF:$\alpha_{IIb}\beta_3$ binding assay provides new tools to advance research on VWF-platelet biology and VWD. These tools could enhance the diagnosis and treatment of bleeding disorders by improving our understanding of platelet function and VWF's role in hemostasis and thrombosis. Future studies will investigate the therapeutic potential of targeting VWF-$\alpha_{IIb}\beta_3$ interactions in bleeding and thrombotic disorders.

Disclosures

No conflicts of interest to disclose.

Contributions

QS designed experiments, analyzed data, and wrote the manuscript. JGM, PAM, PAC, JAS and SAF designed and performed experiments, analyzed data, and edited the manuscript. JR maintained mouse colonies and performed genotyping. MLS helped with the laser injury model study. JZ provided critical reagents and edited the manuscript. HW helped to generate VWF-RGES mouse model. SLH helped in designing research. VHF helped in designing research and edited the manuscript. RRM designed and supervised research, and edited the manuscript.

Acknowledgments

We thank Dr. Mathew Flick at the University of North Carolina at Chapel Hill for providing fibrinogen knockout and γΔ5 variant mice. We thank Dr. Peter Newman at the Versiti Blood Research Institute for providing HEK293F cells stably expressing murine $\alpha_{IIb}\beta_3$. We thank the Zimmerman Program investigators and participating clinical hematology centers (see Online Supplementary Appendix). The authors thank the Versiti Blood Research Institute Shared Resources (RRID: SCR_025503) for their services, instrumentation, and specialist support.

Funding

This work was supported by the National Heart, Lung, and Blood Institute, National Institutes of Health grants HL139847 (to RRM), HL081588 (to RRM), HL144457 (to RRM), HL112614 (to RRM), and HL102035 (to QS), and support from the Versiti Blood Research Foundation, the Children's Hospital of Wisconsin Foundation (to QS), the Midwest Athletes Against Childhood Cancer and Bleeding Disorders Fund (to QS).

Data-sharing statement

The authors confirm that the data supporting the findings of this study are available within the article and/or its Online Supplementary Appendix. For additional information, please contact the corresponding author.

References

1. Lenting PJ, Denis CV, Christophe OD. Von Willebrand factor: how unique structural adaptations support and coordinate its complex function. Blood. 2024;144(21):2174-2184.
2. Bryckaert M, Rosa JP, Denis CV, Lenting PJ. Of von Willebrand factor and platelets. Cell Mol Life Sci. 2015;72(2):307-326.
3. Brill A, Fuchs TA, Chauhan AK, et al. von Willebrand factor-mediated platelet adhesion is critical for deep vein thrombosis in mouse models. Blood. 2011;117(4):1400-1407.
4. Reininger AJ. Function of von Willebrand factor in haemostasis and thrombosis. Haemophilia. 2008;14(Suppl 5):11-26.
5. Kasirer-Friede A, Cozzi MR, Mazzucato M, De Marco L, Ruggeri ZM, Shattil SJ. Signaling through GP Ib-IX-V activates alpha IIb beta 3 independently of other receptors. Blood. 2004;103(9):3403-3411.
6. Reininger AJ, Heijnen HF, Schumann H, Specht HM, Schramm W, Ruggeri ZM. Mechanism of platelet adhesion to von Willebrand factor and microparticle formation under high shear stress. Blood. 2006;107(9):3537-3545.
7. Nesbitt WS, Kulkarni S, Giuliano S, et al. Distinct glycoprotein Ib/V/IX and integrin alpha IIbbeta 3-dependent calcium signals cooperatively regulate platelet adhesion under flow. J Biol Chem. 2002;277(4):2965-2972.
8. Plow EF, McEver RP, Coller BS, Woods VL Jr, Marguerie GA, Ginsberg MH. Related binding mechanisms for fibrinogen, fibronectin, von Willebrand factor, and thrombospondin on thrombin-stimulated human platelets. Blood. 1985;66(3):724-727.
9. Schullek J, Jordan J, Montgomery RR. Interaction of von Willebrand factor with human platelets in the plasma milieu. J Clin Invest. 1984;73(2):421-428.
10. Nachman RL, Leung LL. Complex formation of platelet membrane glycoproteins IIb and IIIa with fibrinogen. J Clin Invest. 1982;69(2):263-269.
11. Adelman B, Carlson P, Powers P. von Willebrand factor is present on the surface of platelets stimulated in plasma by ADP. Blood. 1987;70(5):1362-1366.
12. Pieters M, Wolberg AS. Fibrinogen and fibrin: an illustrated review. Res Pract Thromb Haemost. 2019;3(2):161-172.
13. Springer TA. von Willebrand factor, Jedi knight of the bloodstream. Blood. 2014;124(9):1412-1425.
14. Tovar-Lopez FJ, Rosengarten G, Westein E, et al. A microfluidics device to monitor platelet aggregation dynamics in response to strain rate micro-gradients in flowing blood. Lab Chip. 2010;10(3):291-302.
15. Konig G, Obser T, Marggraf O, et al. Alteration in GPIIb/IIIa binding of VWD-associated von Willebrand factor variants with C-terminal missense mutations. Thromb Haemost. 2019;119(7):1102-1111.
16. Montgomery RR, Flood VH. What have we learned from large population studies of von Willebrand disease? Hematology Am

Soc Hematol Educ Program. 2016;2016(1):670-677.
17. Rodeghiero F, Tosetto A, Abshire T, et al. ISTH/SSC bleeding assessment tool: a standardized questionnaire and a proposal for a new bleeding score for inherited bleeding disorders. J Thromb Haemost. 2010;8(9):2063-2065.
18. Christopherson PA, Tijet N, Haberichter SL, et al. The common VWF variant p.Y1584C: detailed pathogenic examination of an enigmatic sequence change. J Thromb Haemost. 2024;22(3):666-675.
19. Sadler B, Christopherson PA, Haller G, Montgomery RR, Di Paola J. von Willebrand factor antigen levels are associated with burden of rare nonsynonymous variants in the VWF gene. Blood. 2021;137(23):3277-3283.
20. Zhu J, Zhu J, Negri A, et al. Closed headpiece of integrin alphaIIbbeta3 and its complex with an alphaIIbbeta3-specific antagonist that does not induce opening. Blood. 2010;116(23):5050-5059.
21. Beacham DA, Wise RJ, Turci SM, Handin RI. Selective inactivation of the Arg-Gly-Asp-Ser (RGDS) binding site in von Willebrand factor by site-directed mutagenesis. J Biol Chem. 1992;267(5):3409-3415.
22. Shi Q, Fahs SA, Mattson JG, et al. A novel mouse model of type 2N VWD was developed by CRISPR/Cas9 gene editing and recapitulates human type 2N VWD. Blood Adv. 2022;6(9):2778-2790.
23. Suh TT, Holmback K, Jensen NJ, et al. Resolution of spontaneous bleeding events but failure of pregnancy in fibrinogen-deficient mice. Genes Dev. 1995;9(16):2020-2033.
24. Holmback K, Danton MJ, Suh TT, Daugherty CC, Degen JL. Impaired platelet aggregation and sustained bleeding in mice lacking the fibrinogen motif bound by integrin alpha IIb beta 3. EMBO J. 1996;15(21):5760-5771.
25. Shi Q, Fahs SA, Kuether EL, Cooley BC, Weiler H, Montgomery RR. Targeting FVIII expression to endothelial cells regenerates a releasable pool of FVIII and restores hemostasis in a mouse model of hemophilia A. Blood. 2010;116(16):3049-3057.
26. Shi Q, Schroeder JA, Kuether EL, Montgomery RR. The important role of von Willebrand factor in platelet-derived FVIII gene therapy for murine hemophilia A in the presence of inhibitory antibodies. J Thromb Haemost. 2015;13(7):1301-1309.
27. Flood VH, Schlauderaff AC, Haberichter SL, et al. Crucial role for the VWF A1 domain in binding to type IV collagen. Blood. 2015;125(14):2297-2304.
28. Flood VH, Gill JC, Christopherson PA, et al. Comparison of type I, type III and type VI collagen binding assays in diagnosis of von Willebrand disease. J Thromb Haemost. 2012;10(7):1425-1432.
29. Slobodianuk TL, Kochelek C, Foeckler J, Kalloway S, Weiler H, Flood VH. Defective collagen binding and increased bleeding in a murine model of von Willebrand disease affecting collagen IV binding. J Thromb Haemost. 2019;17(1):63-71.
30. Zhang G, Shi Q, Fahs SA, Kuether EL, Walsh CE, Montgomery RR. Factor IX ectopically expressed in platelets can be stored in alpha-granules and corrects the phenotype of hemophilia B mice. Blood. 2010;116(8):1235-1243.
31. Baumgartner CK, Zhang G, Kuether EL, Weiler H, Shi Q, Montgomery RR. Comparison of platelet-derived and plasma factor VIII efficacy using a novel native whole blood thrombin generation assay. J Thromb Haemost. 2015;13(12):2210-2219.
32. Kanaji S, Fahs SA, Shi Q, Haberichter SL, Montgomery RR. Contribution of platelet vs. endothelial VWF to platelet adhesion and hemostasis. J Thromb Haemost. 2012;10(8):1646-1652.
33. Johansen PB, Tranholm M, Haaning J, Knudsen T. Development of a tail vein transection bleeding model in fully anaesthetized haemophilia A mice - characterization of two novel FVIII molecules. Haemophilia. 2016;22(4):625-631.
34. Chen Y, Schroeder JA, Kuether EL, Zhang G, Shi Q. Platelet gene therapy by lentiviral gene delivery to hematopoietic stem cells restores hemostasis and induces humoral immune tolerance in FIX(null) mice. Mol Ther. 2014;22(1):169-177.
35. Kim KH, Barazia A, Cho J. Real-time imaging of heterotypic platelet-neutrophil interactions on the activated endothelium during vascular inflammation and thrombus formation in live mice. J Vis Exp. 2013:(74):50329.
36. Neyman M, Gewirtz J, Poncz M. Analysis of the spatial and temporal characteristics of platelet-delivered factor VIII-based clots. Blood. 2008;112(4):1101-1108.
37. Flood VH, Gill JC, Friedman KD, et al. Collagen binding provides a sensitive screen for variant von Willebrand disease. Clin Chem. 2013;59(4):684-691.
38. Christopherson PA, Haberichter SL, Flood VH, et al. Ristocetin dependent cofactor activity in von Willebrand disease diagnosis: limitations of relying on a single measure. Res Pract Thromb Haemost. 2022;6(7):e12807.
39. Shi Q, Kuether EL, Schroeder JA, Fahs SA, Montgomery RR. Intravascular recovery of VWF and FVIII following intraperitoneal injection and differences from intravenous and subcutaneous injection in mice. Haemophilia. 2012;18(4):639-646.
40. Baumgartner CK, Mattson JG, Weiler H, Shi Q, Montgomery RR. Targeting factor VIII expression to platelets for hemophilia A gene therapy does not induce an apparent thrombotic risk in mice. J Thromb Haemost. 2017;15(1):98-109.
41. Seidizadeh O, Eikenboom JCJ, Denis CV, et al. von Willebrand disease. Nat Rev Dis Primers. 2024;10(1):51.
42. Kalot MA, Husainat N, Abughanimeh O, et al. Laboratory assays of VWF activity and use of desmopressin trials in the diagnosis of VWD: a systematic review and meta-analysis. Blood Adv. 2022;6(12):3735-3745.
43. Veyradier A, Jumilly AL, Ribba AS, et al. New assay for measuring binding of platelet glycoprotein IIb/IIIa to unpurified von Willebrand factor. Thromb Haemost. 1999;82(1):134-139.
44. Schneppenheim R, Hellermann N, Brehm MA, et al. The von Willebrand factor Tyr2561 allele is a gain-of-function variant and a risk factor for early myocardial infarction. Blood. 2019;133(4):356-365.
45. Ruggeri ZM. Platelet and von Willebrand factor interactions at the vessel wall. Hamostaseologie. 2004;24(1):1-11.
46. Huck V, Chen PC, Xu ER, et al. Gain-of-function variant p.Pro2555Arg of von Willebrand factor increases aggregate size through altering stem dynamics. Thromb Haemost. 2022;122(2):226-239.
47. Tomaiuolo M, Brass LF, Stalker TJ. Regulation of platelet activation and coagulation and its role in vascular injury and arterial thrombosis. Interv Cardiol Clin. 2017;6(1):1-12.
48. Scridon A. Platelets and their role in hemostasis and thrombosis-from physiology to pathophysiology and therapeutic implications. Int J Mol Sci. 2022;23(21):12772.
49. Sang Y, Roest M, de LB, de Groot PG, Huskens D. Interplay between platelets and coagulation. Blood Rev. 2021;46:100733.
50. Croteau SE, Abajas YL, Wolberg AS, et al. Recombinant porcine factor VIII for high-risk surgery in paediatric congenital haemophilia A with high-titre inhibitor. Haemophilia. 2017;23(2):e93-e98.